

Optimizing thermoelectric efficiency of superlattice nanowires at room temperature

David M T Kuo¹, C. C. Chen,² and Yia-Chung Chang^{2,3}

¹*Department of Electrical Engineering and Department of Physics,
National Central University, Chungli, 320 Taiwan*

²*Research Center for Applied Sciences, Academic Sinica, Taipei, 11529 Taiwan and*

³*Department of Physics, National Cheng Kung University, Tainan, 701 Taiwan*

(Dated: November 9, 2018)

It is known that the figure of merit (ZT) of thin nanowires can be significantly enhanced at room temperature due to the reduction of phonon thermal conductance arising from the increase of boundary scattering of phonons. It is expected that the phonon thermal conductance of nanowires filled with quantum dots (QDs) will be further reduced. Here we consider a superlattice nanowire (SLNW) modeled by a linear chain of strongly coupled QDs connected to electrodes. We study the dependence of ZT on the QD energy level (E_0) (relative to the Fermi level E_F in the electrodes), inter-dot coupling strength (t_c), tunneling rate (Γ), and temperature T in order to optimize the design. It is found that at room temperature the maximum power factor occurs when $(E_0 - E_F)/k_B T \approx 2.4$ and $\Gamma = t_c$, a result almost independent of the number of QDs in SLNW as long as $t_c/k_B T < 0.5$. By using reasonable physical parameters we show that thin SLNW with cross-sectional width near 3 nm has a potential to achieve $ZT \geq 3$.

I. INTRODUCTION

Extensive studies have shown that in bulk thermoelectric materials, it is difficult to achieve a figure of merit (ZT) larger than one at room temperature.[1,2] With the advances of nanostructure technology, many experiments nowadays can realize ZT larger than one at room temperature in low-dimensional structures.[3,4] The search of nanostructured materials with significantly improved ZT is still a subject of hot pursuit. If a material with $ZT \geq 3$ at room temperature (which corresponds to a Carnot efficiency around 30% [4]) can be found, it will brighten the scenario of thermoelectric devices tremendously.[1,2] For example, thermoelectric generators (TEGs) using human body as a heat source can be applied to wearable electrical powers, which are very useful for commercial wireless communication and low power electronics[5]. Thermoelectric coolers will also become a viable option for many applications.[1,2] It has been predicted theoretically that $ZT \geq 3$ can be achieved in thin semiconductor nanowires.[6,7] However, no experimental realization of such impressive TE devices has been reported.[1,2]

The finding of $ZT = 1$ in silicon nanowires at room temperature[8] has inspired further studies of thermoelectric properties of silicon-based nanowires because of the advantages of low cost and the availability of matured fabrication technology in silicon industry.[8-10] Whether $ZT \geq 3$ exists in silicon-based nanowires at room temperature becomes an interesting topic. Monte Carlo simulations[11] have demonstrated that in heavily-doped Si nanowires ZT does not increase dramatically with decreasing wire cross section since the electron conductance suffers stronger ionized-impurity scattering as the size reduces. Thus, to improve ZT it is better to use intrinsic nanowires. Silicon nanowire filled with quantum dots (QDs) may provide an alternative means to realize the values of $ZT \geq 1$. [1,2] Furthermore, it is estimated that Si/Ge superlattice nanowire (SLNW) with an opti-

mized period around 5 nm and cross-sectional area around $3\text{ nm} \times 3\text{ nm}$ can lead to a reduction of phonon thermal conductance by one order of magnitude in comparison with pristine Si nanowires.[12,13] Therefore, it is desirable to study the dependence of ZT on relevant physical parameters of Si/Ge SLNWs near room temperature.

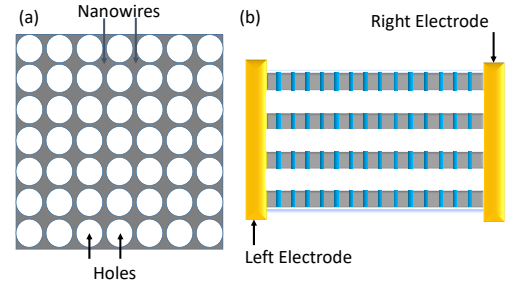


FIG. 1: (a) Schematic sketch of the creation of superlattice nanowires (SLNWs). (b) Side view of SLNWs connected to electrodes.

Here, we perform theoretical calculations of the thermoelectric properties of intrinsic SLNW connected with electrodes by using a linear chain of strongly coupled QDs. The electron carriers in SLNWs are provided by metallic electrodes with Fermi level below the conduction band minimum as proposed in[14]. The SLNW structure can be realized by starting with a superlattice with optimized period to minimize the phonon thermal conductance. The creation of nanowires may be achieved by lithographically drilling a periodic array of closely-spaced holes[10], leaving an array of nanowires (with a star-shaped cross-section) as depicted in Fig. 1. To re-

duce the electron scattering from the rough surface, the side surfaces of the nanowires are oxidized to form a high electron barrier, which serves the purpose of confining electrons in the central region of the star-shaped nanowires. Due to the strong confinement of electrons, the electron-surface scattering can be reduced. At the same time the acoustic phonons are not so well confined in the central region which will then suffer more surface scattering. With such a design, we found that $ZT \geq 3$ may be achieved in a thin SLNW with reasonable physical parameters adopted. Our theoretical studies should provide a useful guideline for the design of future thermoelectric devices operating at room temperature.

II. FORMALISM

To model the thermoelectric properties of SLNWs, we consider a linear chain of strongly-coupled QDs with a system Hamiltonian given by an Anderson model $H = H_0 + H_{QD}$, [15] where

$$H_0 = \sum_{k,\sigma} \epsilon_k a_{k,\sigma}^\dagger a_{k,\sigma} + \sum_{k,\sigma} \epsilon_k b_{k,\sigma}^\dagger b_{k,\sigma} \quad (1)$$

$$+ \sum_{k,\sigma} V_{k,L}^L d_{L,\sigma}^\dagger a_{k,\sigma} + \sum_{k,\sigma} V_{k,R}^R d_{R,\sigma}^\dagger b_{k,\sigma} + c.c.$$

The first two terms of Eq. (1) describe the free electron gas in the left and right electrodes. $a_{k,\sigma}^\dagger$ ($b_{k,\sigma}^\dagger$) creates an electron of momentum k and spin σ with energy ϵ_k in the left (right) electrode. $V_{k,L}^L$ ($V_{k,R}^R$) describes the coupling between the left (right) lead with its adjacent QD. $d_{L(R),\sigma}^\dagger$ ($d_{L(R),\sigma}$) creates (destroys) an electron in the QD connected to the left (right) lead.

$$H_{QD} = \sum_{\ell,\sigma} E_\ell d_{\ell,\sigma}^\dagger d_{\ell,\sigma} + \sum_{\ell \neq j} t_{\ell,j} d_{\ell,\sigma}^\dagger d_{j,\sigma}, \quad (2)$$

where E_ℓ is the QD energy level in the ℓ -th QD and $t_{\ell,j}$ describes the electron hopping strength between the ℓ -th and j -th QDs. Here, for simplicity, we consider only one energy level for each QD, which is suitable for nanoscale QDs with no valley degeneracy. For example, a cylindrical GaAs QD with high lateral potential barrier resulting from oxidation and vertical confinement via the band onset between GaAs and AlGaAs has a bound state (which is well separated in energy from the excited states) for diameter near 3 nm and height near 5 nm. [16] For silicon QDs in the Si/Ge SLNW, we expect the valley degeneracy to lead to enhanced density of states in the energy range of interest, which can actually improve ZT further. [17] It should be noted that the Hubbard-like terms for Coulomb interactions between electrons in the SLNWs are neglected, since the electrons are delocalized along the transport direction in the strong hopping limit considered.

To study the transport properties of QDs junction connected with electrodes, it is convenient to use the Green-function technique. The electron and heat currents from

reservoir α to its adjacent QD are calculated according to the Meir-Wingreen formula [18]

$$J_\alpha^n = \frac{ie}{h} \sum_{j\sigma} \int d\epsilon \left(\frac{\epsilon - \mu_\alpha}{e} \right)^n \Gamma_\alpha(\epsilon) [G_{\alpha,\sigma}^<(\epsilon) \quad (3)$$

$$+ f_\alpha(\epsilon) (G_{\alpha,\sigma}^r(\epsilon) - G_{\alpha,\sigma}^a(\epsilon))],$$

where $n = 0$ is for the electrical current and $n = 1$ for the heat current. $\Gamma_{L(R)}(\epsilon) = \sum_k |V_{k,L(R)}|^2 \delta(\epsilon - \epsilon_k)$ is the tunneling rate for electrons from the left (right) reservoir and entering the left (right) QD. $f_\alpha(\epsilon) = 1/\{\exp[(\epsilon - \mu_\alpha)/k_B T_\alpha] + 1\}$ denotes the Fermi distribution function for the α -th electrode, where μ_α and T_α are the chemical potential and the temperature of the α electrode. e , h , and k_B denote the electron charge, the Planck's constant, and the Boltzmann constant, respectively. $G_{\alpha,\sigma}^<(\epsilon)$, $G_{\alpha,\sigma}^r(\epsilon)$, and $G_{\alpha,\sigma}^a(\epsilon)$ denote the frequency-domain representations of the one-particle lesser, retarded, and advanced Green's functions, respectively.

In the linear response regime electrical conductance (G_e), Seebeck coefficient (S) and electron thermal conductance (κ_e) can be evaluated by using Eq. (3) with a small applied bias $\Delta V = (\mu_L - \mu_R)/e$ and temperature difference across junction $\Delta T = T_L - T_R$. [17] For simplicity, we calculate these thermoelectric coefficients in terms of Landauer formula [19,20]. Here we have $G_e = e^2 \mathcal{L}_0$, $S = -\mathcal{L}_1/(eT\mathcal{L}_0)$ and $\kappa_e = \frac{1}{T}(\mathcal{L}_2 - \mathcal{L}_1^2/\mathcal{L}_0)$. Thermoelectric coefficients \mathcal{L}_n are given by

$$\mathcal{L}_n = \frac{2}{h} \int d\epsilon \mathcal{T}_{LR}(\epsilon) (\epsilon - E_F)^n \frac{\partial f(\epsilon)}{\partial E_F}, \quad (4)$$

where $f(\epsilon) = 1/(\exp[(\epsilon - E_F)/k_B T] + 1)$ is the Fermi distribution function of electrodes at equilibrium temperature T and $\mathcal{T}_{LR}(\epsilon)$ is the transmission coefficient. E_F is the Fermi energy of electrodes. The expression of $\mathcal{T}_{LR}(\epsilon)$ in Eq. (4) is given by [20,21]

$$\mathcal{T}_{LR}(\epsilon) = \frac{-4\Gamma_L \Gamma_R^{eff}(\epsilon)}{\Gamma_L + \Gamma_R^{eff}(\epsilon)} \text{Im}(G_L^r(\epsilon)), \quad (5)$$

where $G_L^r(\epsilon) = 1/(\epsilon - E_1 + i\Gamma_L - \Sigma_{1,N}(\epsilon))$ denotes the one-particle retarded Green function of the leftmost QD with the energy level of E_1 , in which the self energy $\Sigma_{1,N}(\epsilon)$ resulting from electron tunneling from the leftmost QD to the right electrode mediated by $N-1$ QDs is given by [21]

$$\Sigma_{1,N}(\epsilon) = \frac{t_{1,2}^2}{\epsilon - E_2 - \frac{t_{2,3}^2}{\epsilon - E_3 - \dots - \frac{t_{N-1,N}^2}{\epsilon - E_N + i\Gamma_R}}}, \quad (6)$$

where N denotes the total number of QDs. The rightmost QD is the N th QD. The effective tunneling rate $\Gamma_R^{eff} = -\text{Im}(\Sigma_{1,N}(\epsilon))$. For simplicity, we assume $E_\ell = E_0$ and $t_{\ell,j} = t_c$ for all ℓ and j being the nearest neighbor of ℓ , and $\Gamma_L = \Gamma_R \equiv \Gamma$.

The figure of merit $ZT = S^2 G_e T / (\kappa_e + \kappa_{ph})$ contains the phonon thermal conductance (κ_{ph}) of SLNW, which

can not be neglected at room temperature.[17] Many theoretical efforts have been devoted to the study of phonon thermal conductance of silicon nanowires.[22,23] Here, we adopt the formula of phonon thermal conductance as given in Ref. [23], which can well describe the experimental results of Si nanowires.[23,24] We have

$$\kappa_{ph,0}(T) = \frac{1}{h} \int d\omega \mathcal{T}(\omega)_{ph} \frac{\hbar^3 \omega^2}{k_B T^2} \frac{e^{\hbar\omega/k_B T}}{(e^{\hbar\omega/k_B T} - 1)^2}, \quad (7)$$

where ω is the phonon frequency and $\mathcal{T}_{ph}(\omega)$ the throughput function. In [12,13,25] it is theoretically demonstrated that $\kappa_{ph}(T)$ of Si nanowires filled with QDs is significantly reduced from the value $\kappa_{ph,0}(T)$ for Si nanowires without QDs for a wide range of temperatures. To simulate the phonon thermal conductance of SLNWs (which is filled with QDs), we use a simple expression $\kappa_{ph}(T) = F_s \kappa_{ph,0}(T)$, where F_s is a dimensionless scaling factor used to describe the phonon scattering resulting from the interface scattering of QDs, a filtering mechanism for short wavelength acoustic phonons.[12,13] Values of F_s can range from 0.1 to 1.[12,13,25] It is well known that QD size fluctuation and surface roughness will also degrade the electron transport[26,27] For simplicity, we assume that the electrical conductance and thermal conductance due to electron-phonon scattering and electron scattering from the surface roughness and QD size fluctuation can be modeled by a same scaling factor $F_e = 1/(1 + L/\lambda)$, where L and λ denote the channel length and electron mean free path, respectively. Namely, the electrical conductance and thermal conductance for realistic SLNWs are expressed as $G'_e = F_e G_e$ and $\kappa'_e = F_e \kappa_e$, respectively. The resulting ZT now reads $ZT = S^2 G_e T / (\kappa_e + \kappa_{ph,0} f_s)$, where $f_s = F_s / F_e$. For an optimized design of SLNW as illustrated in Fig. 1, it is conceivable that f_s can be less than 1. F_e is roughly proportional to the ratio of mean-free path to the channel length. The mean-free path of electrons in germanium/silicon nanowires reported is beyond 170nm at room temperature.[27] Thus, $F_e \approx 0.2$ for a micron size SLNW considered here, and the best value of f_s can be expected is around 0.5. Taking the possible size nonuniformity of QDs into account, we shall consider the value of f_s to be between 0.7 and 1 in our simulation and examine what values of ZT can be achieved for SLNWs.

III. RESULTS AND DISCUSSION

Before discussing the optimization of ZT at room temperature, we first study the power factor ($PF = S^2 G_e$) of SLNWs as a function of system parameters such as QD energy level (relative to E_F) and the tunneling rate (Γ), since the behavior of ZT is mostly determined by PF in the limit $\kappa_{ph}/\kappa_e \gg 1$. Figure 2 shows the electrical conductance, Seebeck coefficient and power factor as functions of QD energy level (E_0) relative to the Fermi level (E_F) at two different temperatures. All energy scales are in units of Γ_0 , which is taken to be 1 meV. In the strong-hopping limit, $t_c/\Gamma \gg 1$, the expression of $\mathcal{T}_{LR}(\epsilon)$ can be

approximated by

$$\mathcal{T}_{LR}(\epsilon) = \Pi_n^N \frac{4\Gamma^2 (t_c^2)^{N-1}}{(\epsilon - [E_0 - 2t_c \cos(\frac{n\pi}{N+1})])^2 + (\Gamma_n)^2}, \quad (8)$$

where $\Gamma_n = \Gamma \sqrt{2/(N+1)} \sin(\frac{n\pi}{N+1})$ for $n = 1, \dots, N$. At low temperature ($k_B T = 1\Gamma_0$), the behavior of G_e can be roughly described by $\mathcal{T}_{LR}(E_F)$, which is nonzero only when E_F falls within the SLNW band, which covers the range from -32 to $32\Gamma_0$, since the band width is $4t_c = 64\Gamma_0$. [See Fig. 2(a)] The G_e spectrum becomes significantly broadened near room temperature with $k_B T = 25\Gamma_0$. The enhancement of G_e outside the SLNW band is due to the thermionic effect.[14] As seen in Fig. 2(b), the Seebeck coefficient S is an antisymmetric function of $\Delta = E_0 - E_F$. Such a bipolar behavior has been reported in several studies.[19,21] The negative sign of S indicates the main contribution coming from electrons tunnel through the resonant channels of the band above the Fermi level, while the positive sign of S indicates the main contribution coming from holes tunneling through the band below E_F . As seen in Fig. 2(c) the PF spectrum shows two strong peaks when E_F is near the SLNW band edges at low temperature, and the peaks are broadened and shifted away from the band region as temperature increases.

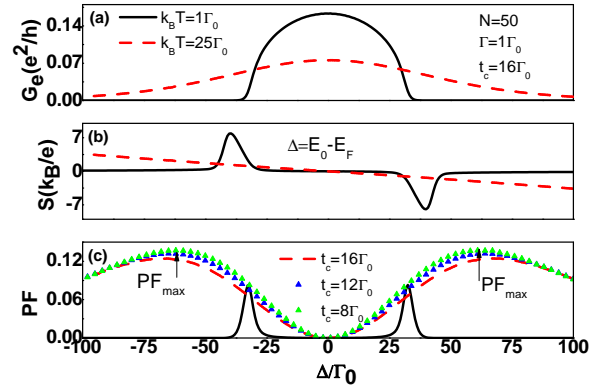


FIG. 2: (a) Electrical conductance, (b) Seebeck coefficient and (c) power factor ($PF = S^2 G_e$) as a function of $\Delta = E_0 - E_F$ for two different temperatures in an SLNW junction with electron hopping strengths $t_c = 16\Gamma_0$. In (c) we also add results for $t_c = 8$ and $12\Gamma_0$ (triangles) at $k_B T = 25\Gamma_0$. Other parameters used are $\Gamma_L = \Gamma_R = \Gamma = 1\Gamma_0$ and $N = 50$.

To find the maximum of PF at room temperature ($k_B T = 25\Gamma_0$), we also calculate PF as a function of Δ for various coupling strengths. It is found that the maximum PF occurs near $\Delta = 60\Gamma_0 = 2.4k_B T$. Interestingly, this feature is nearly independent of the number of QDs in SLNW as long as $t_c/k_B T$ is small.

Let's consider the case of $N = 2$, which has an analytical solution. We have

$$\mathcal{T}_{LR}(\epsilon) = \frac{4\Gamma_L \Gamma_R t_c^2}{|(\epsilon - E_0 + i\Gamma_L)(\epsilon - E_0 + i\Gamma_R) - t_c^2|^2}. \quad (9)$$

Under the assumption of $\Gamma/k_B T \ll t_c/k_B T \ll 1$, we have

$$\mathcal{L}_0 = \frac{1}{hk_B T} \frac{\pi \Gamma t_c^2}{2(t_c^2 + (\Gamma/2)^2)} \frac{1}{\cosh^2(\frac{\Delta}{2k_B T})} \quad (10)$$

and

$$\mathcal{L}_1 = \frac{1}{hk_B T} \frac{\pi \Gamma t_c^2}{2(t_c^2 + (\Gamma/2)^2)} \frac{\Delta}{\cosh^2(\frac{\Delta}{2k_B T})}. \quad (11)$$

From Eqs. (10) and (11), we get $S = -\frac{\Delta}{eT}$ which explains the linear behavior of S at $k_B T = 25\Gamma_0$ in Fig. 2(b). Furthermore,

$$PF = \frac{(\Delta/eT)^2 G_0}{k_B T} \frac{\pi \Gamma t_c^2}{2(t_c^2 + (\Gamma/2)^2)} \frac{1}{\cosh^2(\frac{\Delta}{2k_B T})}, \quad (12)$$

where $G_0 = e^2/h$ denotes the electron quantum conductance. The above equation gives a maximum PF at $\Delta/k_B T = 2.4$. This result holds well for any number of N (tested up to $N = 100$) as long as $t_c/k_B T < 0.5$.

In Fig. 2, we have considered the case with $\Gamma = 1\Gamma_0$. Next, we study how the thermoelectric properties of SLNW are affected by increasing the tunneling rate Γ . Figure 3 shows the calculated G_e , S and PF as functions of Γ for various values of t_c at the optimum condition with $\Delta = 2.4k_B T = 60\Gamma_0$. The Γ dependence of PF is dominated by G_e since S is almost independent of Γ as can be seen in Fig. 3(b). It is found that the maximum PF occurs when $\Gamma = t_c$, as indicated by arrows in Fig. 3(c). We found this relation also holds approximately for any value of N . For comparison, we also add the results obtained by Eq. (9) for $N = 2$ (curves with triangle).[28]

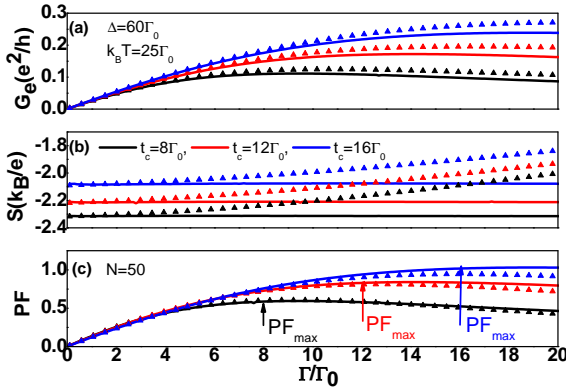


FIG. 3: (a) Electrical conductance G_e , (b) Seebeck coefficient S , and (c) power factor (PF) as a function of electron tunneling rate Γ for various t_c at $k_B T = 25\Gamma_0$. Solid curves are for $N = 50$. Triangles are obtained by Eq. (9) for $N=2$. Other physical parameters are the same as those of Fig. 2.

Although previous theoretical studies have predicted high ZT values of QD junctions in the Coulomb blockade regime [19] for the case of $\kappa_e \gg \kappa_{ph}$, it is valid only at extremely low temperature. To illustrate the importance of κ_{ph} , we show in Fig. 4 κ_e and $\kappa_{ph,0}$ as functions of

temperature at $\Delta = 60\Gamma_0$ and $\Gamma = t_c$. As seen in Fig. 4(a) κ_e reaches a maximum at 300 K and the maximum value is enhanced with increasing t_c or Γ . Here we have adopted the optimum case with $\Gamma = t_c$. For the Si/Ge superlattice with an optimized period of 5 nm, the SLNW with $N = 200$ has a length of $L = 1000$ nm. Therefore, we are interested in κ_{ph} of nanowires with length of $L = 1000$ nm. The calculated $\kappa_{ph,0}$ based on Eq. 7 for silicon nanowires with surface roughness width $\delta = 2$ nm and $L = 1000$ nm are shown in Fig. 4(b) for three different diameters ($D = 3, 4, 5$ nm). The magnitude of κ_{ph} is reduced very quickly when D is reduced. We find that $\kappa_{ph,0}$ is larger than κ_e at $T = 300$ K even though for the $D = 3$ nm. Both κ_e and κ_{ph} will be included in the calculation of ZT .

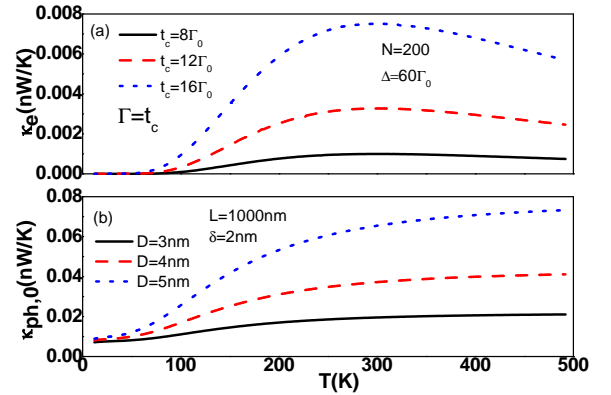


FIG. 4: (a) Electron thermal conductance κ_e of SLNW with $N=200$ and (b) phonon thermal conductance of nanowires with diameters of 3, 4, and 5 nm as functions of temperature.

The calculated ZT as a function of temperature for various values of f_s is shown in Fig. 5. The optimum condition $\Delta = 60\Gamma_0$ has been used. It is seen in Fig. 5(a) that ZT can reach 3 at $T = 300$ K with $t_c \geq 12\Gamma_0$ even with $f_s = 1$. If we assume that phonons suffer more scattering from QDs than electrons (i.e. $f_s < 1$) as implied in previous studies,[12,13,25] the resulting ZT of SLNWs can be further enhanced as illustrated in Fig. 5(b) for $t_c = \Gamma = 16\Gamma_0$. The value of ZT can be larger than 3 over a wide temperature range. This feature can be very useful for the application of TEG at room temperature.

Finally, we examine the dependence of ZT on the hopping strength, t_c (which controls the SLNW band width) for a few values of Δ around the optimum condition. The behaviors of PF , κ_e and ZT for SLNWs as functions of t_c ($=\Gamma$) are shown in Fig. 6. It is found that ZT reaches a maximum around $t_c = \Gamma = 16\Gamma_0$, while both G_e and κ_e continue to increase with increasing t_c ($=\Gamma$). The rate of increase for κ_e surpasses that for PF at $t_c = 15\Gamma_0$, leading to an optimized condition for ZT at that value. In Fig. 6(c), we found that for $t_c > 10\Gamma_0$, the optimum condition for Δ increases slightly with the best value occurring at $\Delta = 70\Gamma_0$. The main reason for the shift of

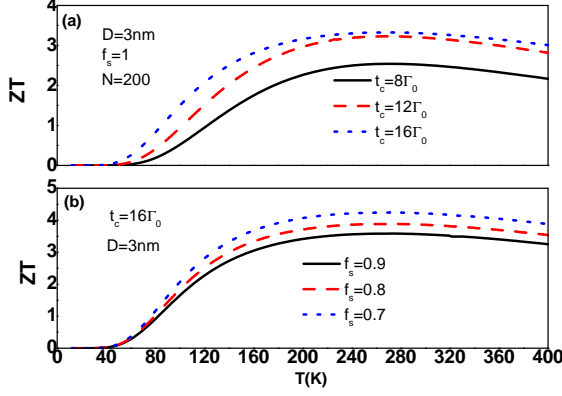


FIG. 5: ZT as a function of temperature. (a) For different values of $t_c (= \Gamma)$ and $f_s = 1$. (b) For different values of f_s with both $t_c = \Gamma$ fixed at $16\Gamma_0$. $\Delta = E_0 - E_F = 60\Gamma_0$ and $D = 3 \text{ nm}$.

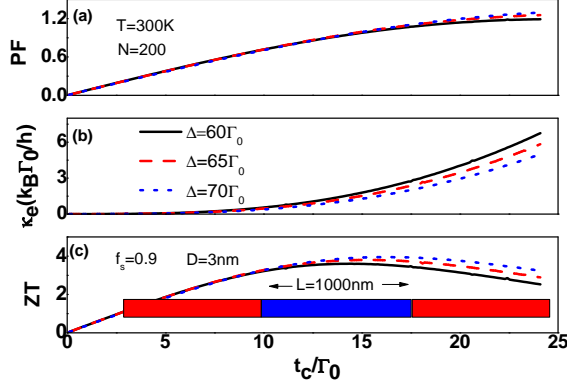


FIG. 6: (a) Power factor, (b) electron thermal conductance and (c) figure of merit (ZT) as functions of electron hopping strength (t_c) for three values of Δ at $T = 300 \text{ K}$ and $N = 200$. Other physical parameters are the same as those of Fig. 5.

optimum value of Δ at large t_c is due to the decrease of κ_e for increasing Δ as seen in Fig. 6(b).

IV. CONCLUSION

We have theoretically studied the thermoelectric properties of SLNWs connected to electrodes at room temperature. At higher temperatures (including room temperature) with $k_B T$ much greater than t_c and Γ , we find the Seebeck coefficient can be approximately described by a linear relation $S = -\Delta/(eT)$ and the maximum of the power factor occurs at $\Delta = 2.4k_B T$. In addition, both the electrical conductance and power factor are maximized under the condition $t_c = \Gamma$ for Δ fixed around $2.4k_B T$. ZT behavior is dominated by PF when $\kappa_{ph} \gg \kappa_e$. However, for large t_c and Γ , κ_e becomes significant and the maximum ZT is determined not only by $PF = S^2 G_e$, but also by κ_e . All the above results are almost independent of the number of QDs in the SLNW. For thin Si/Ge SLNWs with diameter around 3 nm , we find that it may be possible to achieve a ZT larger 3 when the reduction of phonon thermal conductivity due to scattering from QDs is more severe than the reduction of electron conductivity. The linear chain model used here did not take into account the valley degeneracy and excited states of QDs. Adding these will provide more channels for electron conduction, which should improve ZT further.[17] A realistic modeling taking into account the multi-valley band structures of Si and Ge will be left for future investigations.

Acknowledgments

This work was supported under Contract Nos. MOST 106-2112-M-008 -014 and MOST 104-2112-M-001-009 YM2.

E-mail address: mtkuo@ee.ncu.edu.tw

E-mail address: yiachang@gate.sinica.edu.tw

- ¹ G. Chen, M. S. Dresselhaus, G. Dresselhaus, J. P. Fleurial and T. Caillat, *International Materials Reviews*, **48**, 45 (2003).
- ² A. J. Minnich, M. S. Dresselhaus, Z. F. Ren and G. Chen, *Energy Environ Sci*, **2**, 466 (2009).
- ³ R. Venkatasubramanian, E. Siivola, T. Colpitts, B. O'Quinn, *Nature* **413**, 597 (2001).
- ⁴ T. C. Harman, P. J. Taylor, M. P. Walsh, B. E. LaForge, *Science* **297**, 2229 (2002).
- ⁵ F. Suarez, A. Nozariasbmarz, D. Vashaee and M. C. Ozturk, *Energy Environ Sci*, **9**, 2099 (2016).
- ⁶ L. D. Hicks, and M. S. Dresselhaus, *Phys. Rev. B* **47**, 16631 (1993).
- ⁷ N. Mingo, *Appl. Phys. Lett.* **85**, 5986 (2004).
- ⁸ A. I. Boukai, Y. Bunimovich, J. Tahir-Kheli, J. K. Yu, W.

- A. Goddard III and J. R. Heath, *Nature*, **451**, 168 (2008).
- ⁹ A. I. Hochbaum, R. K. Chen, R. D. Delgado, W. J. Liang, E. C. Garnett, M. Najarian, A. Majumdar, and P. D. Yang, *Nature* **451**, 163 (2008).
- ¹⁰ J. H. Lee, J. W. Lim, and P. D. Yang, *Nano Lett.* **15**, 3273 (2015).
- ¹¹ E. B. Ramayya, L. N. Maurer, A. H. Davoody, and I. Knezevic, *Phys. Rev. B* **86**, 115328 (2012).
- ¹² D. L. Nika, E. P. Pokatilov, A. A. Balandin, V. M. Fomin, A. Rastelli, and O. G. Schmidt, *Phys. Rev. B* **84**, 165415 (2011).
- ¹³ Ming Hu and Dimos Poulikakos, *Nano Lett.* **12**, 5487 (2012).
- ¹⁴ G. D. Mahan and L. M. Woods, *Phys. Rev. Lett.* **80**, 4016 (1998).

- ¹⁵ H. Haug and A. P. Jauho, Quantum Kinetics in Transport and Optics of Semiconductors (Springer, Heidelberg, 1996).
- ¹⁶ D. M. T. Kuo, Y. C. Chang, Phys. Rev. B **89** (2014) 115416. 14
- ¹⁷ D. M. T. Kuo, C. C. Chen, and Y. C. Chang, Phys. Rev. B **95**, 075432 (2017).
- ¹⁸ Y. Meir and N. S. Wingreen, Phys. Rev. Lett. **68**, 2512(1992).
- ¹⁹ D. M.-T. Kuo and Y. C. Chang, Phys. Rev. B **81**, 205321 (2010).
- ²⁰ B. H. Teng, H. K. Sy, Z. C. Wang, Y. Q. Sun, and H. C. Yang, Phys. Rev. B **75**, 012105 (2007).
- ²⁶ D. M. T. Kuo and Y. C. Chang, J. Vac. Science and Technology, **31**, 04D108 (2013).
- ²² P. G. Murphy and J. E. Moore, Phys. Rev. B **76**, 155313 (2007).
- ²³ R. K. Chen, A. I. Hochbaum, P. Murphy, J. Moore, P. D. Yang, and A. Majumdar, Phys. Rev. Lett. **101**, 105501 (2008).
- ²⁴ D. Li, Y. Y. Wu, P. Kim, L. Shi, P. D. Yang, and A. Majumdar, Appl. Phys. Lett. **83**, 2934 (2003).
- ²⁵ X. Mu, L. Wang, X. M. Yang, P. Zhang, A. C. To, T. F. Luo, , Scientific Reports **5** 16697 (2015).
- ²⁶ D. M. T. Kuo and Y. C. Chang, Nanotechnology **24**, 175403 (2013).